

# Crackling noise

James P. Sethna\*, Karin A. Dahmen† & Christopher R. Myers‡

\*Laboratory of Atomic and Solid State Physics, Clark Hall, Cornell University, Ithaca, New York 14853-2501, USA (sethna@lassp.cornell.edu)

†Department of Physics, 1110 West Green Street, University of Illinois at Urbana-Champaign, Illinois 61801-3080, USA

(dahmen@physics.uiuc.edu)

‡Cornell Theory Center, Frank H. T. Rhodes Hall, Cornell University, Ithaca, New York 14853-3801, USA (myers@tc.cornell.edu)

**Crackling noise arises when a system responds to changing external conditions through discrete, impulsive events spanning a broad range of sizes. A wide variety of physical systems exhibiting crackling noise have been studied, from earthquakes on faults to paper crumpling. Because these systems exhibit regular behaviour over a huge range of sizes, their behaviour is likely to be independent of microscopic and macroscopic details, and progress can be made by the use of simple models. The fact that these models and real systems can share the same behaviour on many scales is called universality. We illustrate these ideas by using results for our model of crackling noise in magnets, explaining the use of the renormalization group and scaling collapses, and we highlight some continuing challenges in this still-evolving field.**

In the past decade or so, science has broadened its purview to include a new range of phenomena. Using tools developed to understand second-order phase transitions<sup>1–5</sup> in the 1960s and 70s, stochastic models of turbulence<sup>6</sup> in the 1970s, and disordered systems<sup>7–9</sup> in the 1980s, scientists now claim that they should be able to explain how and why things crackle.

Many systems crackle; when pushed slowly, they respond with discrete events of a variety of sizes. The Earth responds<sup>10</sup> with violent and intermittent earthquakes as two tectonic plates rub past one another (Fig. 1). A piece of paper<sup>11</sup> (or a candy wrapper at the cinema<sup>12,15</sup>) emits intermittent, sharp noises as it is slowly crumpled or rumpled. (Try it, but preferably not with this page.) A magnetic material in a changing external field magnetizes in a series of jumps<sup>14,15</sup>. These individual events span many orders of magnitude in size — indeed, the distribution of sizes forms a power law with no characteristic size scale. In the past few years, scientists have been making rapid progress in developing models and theories for understanding this sort of scale-invariant behaviour in driven, nonlinear, dynamical systems.

Interest in these sorts of phenomena goes back several decades. The work of Gutenberg and Richter<sup>10</sup> in the 1940s and 1950s established the well-known frequency-magnitude relationship for earthquakes that bears their names (Fig. 1). A variety of many-degree-of-freedom dynamical models<sup>16–28</sup>, with and without disorder, have been introduced in the years since to investigate the nature of slip complexity in earthquakes. More recent impetus for work in this field came from the study of the depinning transition in sliding charge-density wave (CDW) conductors in the 1980s and early 1990s<sup>29–35</sup>. Interpretation of the CDW depinning transition as a dynamic critical phenomenon sprung from Fisher's early work<sup>29,30</sup>, and several theoretical and numerical studies followed. This activity culminated in the renormalization-group solution by Narayan and Fisher<sup>32</sup> and the numerical studies by Middleton<sup>33</sup> and Myers<sup>34</sup>, which combined to provide a clear picture of depinning in CDWs and open the doors to the study of other disordered, non-equilibrium systems.

Bak, Tang and Wiesenfeld inspired much of the succeeding work on crackling noise<sup>36,37</sup>. They introduced the connection between dynamical critical phenomena and crackling noise, and they emphasized how systems may end

up naturally at the critical point through a process of self-organized criticality. (Their original model was that of avalanches in growing sandpiles — sand has long been used as an example of crackling noise<sup>38,39</sup>, but we now know that real sandpiles do not crackle at the longest scales<sup>40,41</sup>.)

Researchers have studied many systems that crackle. Simple models have been developed to study bubbles rearranging in foams as they are sheared<sup>42</sup>, biological extinctions<sup>43</sup> (where the models are controversial<sup>44,45</sup> — they ignore catastrophic external events like asteroids), fluids invading porous materials and other problems involving invading fronts<sup>46–51</sup> (where the model we describe was invented<sup>46,47</sup>), the dynamics of superconductors<sup>52–54</sup> and superfluids<sup>55,56</sup>, sound emitted during martensitic phase transitions<sup>57</sup>, fluctuations in the stock market<sup>58,59</sup>, solar flares<sup>60</sup>, cascading failures in power grids<sup>61,62</sup>, failures in systems designed for optimal performance<sup>63–65</sup>, group decision-making<sup>66</sup>, and fracture in disordered materials<sup>67–72</sup>. These models are driven systems with many degrees of freedom, which respond to the driving in a series of discrete avalanches spanning a broad range of scales — what in this paper we term crackling noise.

There has been healthy scepticism by some established professionals in these fields to the sometimes-grandiose claims by newcomers claiming support for an overarching paradigm. But often confusion arises because of the unusual kind of predictions the new methods provide. If such models apply at all to a physical system, they should be able to predict most behaviour on long scales of length and time, independent of many microscopic details of the real world. But this predictive capacity comes at a price: the models typically do not make clear predictions of how the real-world microscopic parameters affect the behaviour at long length scales.

Here we provide an overview of the renormalization group<sup>1–5</sup> used by many researchers to understand crackling noise. Briefly, the renormalization group discusses how the effective evolution laws of a system change as measurements are made on longer and longer length scales. (It works by generating a coarse-graining mapping in system space, the abstract space of possible evolution laws.) The broad range of event sizes are attributed to a self-similarity, where the evolution laws look the same at different length scales. This self-similarity leads to a method for scaling experimental data. In the simplest case this yields power laws and fractal

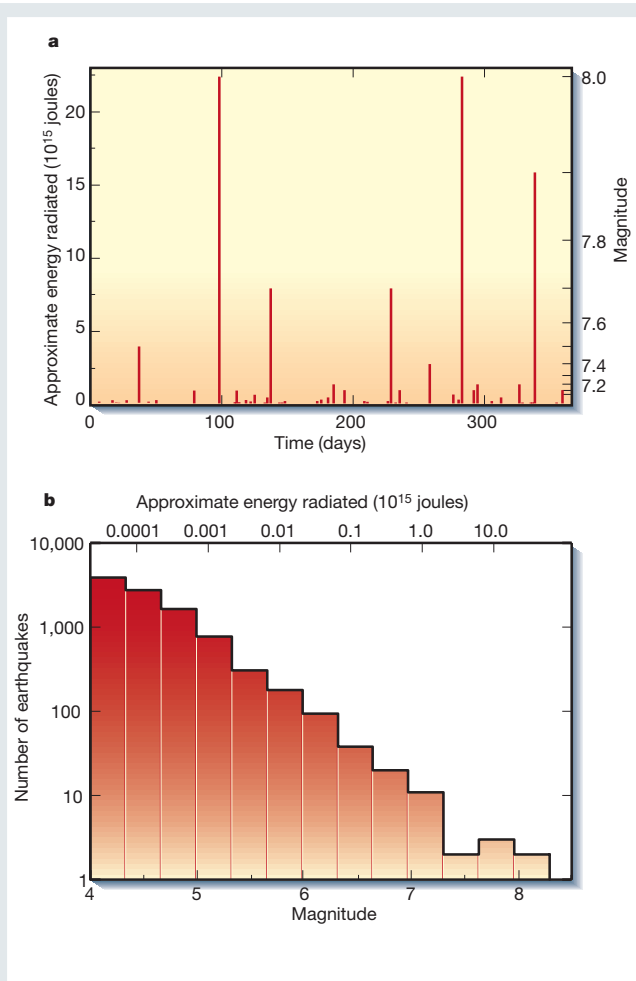


**Figure 1** The Earth crackles. **a**, Time history of radiated energy from earthquakes throughout all of 1995<sup>108–110</sup>. The Earth responds to the slow strains imposed by continental drift through a series of earthquakes (impulsive events well separated in space and time). This time series, when sped up, sounds remarkably like the crackling noise of paper, magnets and Rice Krispies (listen to it in ref. 110). **b**, Histogram of number of earthquakes in 1995 as function of their magnitude (or, alternatively, their energy release). Earthquakes come in a wide range of sizes, from unnoticeable trembles to catastrophic events. The smaller earthquakes are much more common: the number of events of a given size forms a power law<sup>10</sup> called the Gutenberg–Richter law. (Earthquake magnitude scales with the logarithm of the strength of the earthquake. On a log–log plot of number versus radiated energy, the power law is a straight line, as we observe in the plotted histogram.) One would hope that such a simple law should have an elegant explanation.

structures, but more generally it leads to universal scaling functions — where we argue the real predictive power lies. We will only touch upon the complex analytical methods used in this field, but we believe we can explain faithfully and fully both what our tools are useful for, and how to apply them in practice. The renormalization group is perhaps the most impressive use of abstraction in science.

**Why should crackling noise be comprehensible?**

Not all systems crackle. Some respond to external forces with many similar-sized, small events (for example, popcorn popping as it is heated). Others give way in one single event (for example, chalk snapping as it is stressed). In broad terms, crackling noise is in between these limits: when the connections between parts of the system are stronger than in popcorn but weaker than in the grains making up chalk, the yielding events can span many size scales. Crackling forms the transition between snapping and popping.

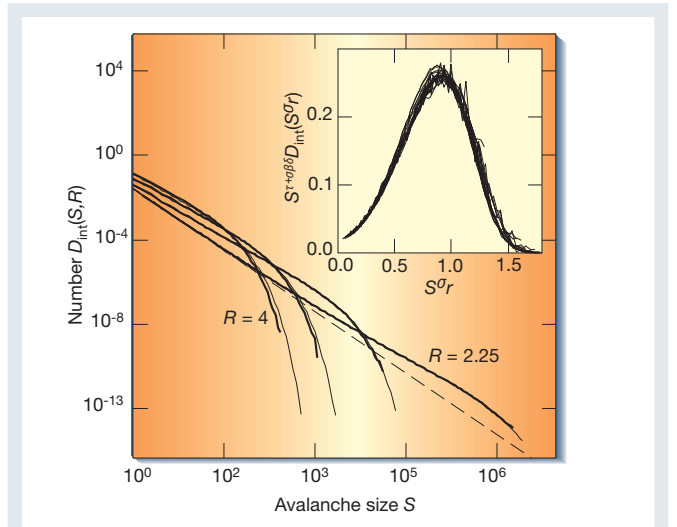


**Figure 2** Magnets crackle<sup>73–76</sup>. Magnets respond to a slowly varying external field by changing their magnetization in a series of bursts, or avalanches. These bursts, called Barkhausen noise, are very similar (albeit on different time and size scales) to those shown in Fig. 1 for earthquakes. The avalanches in our model have a power-law distribution only at a special value of the disorder,  $R_c = 2.16$ . Shown is a histogram giving the number of avalanches  $D_{int}(S, R)$  of a given size  $S$  at various disorders  $R$  ranging from 4 to 2.25; the thin lines are theoretical predictions from our model. ( $D_{int}$  gives all the avalanches during our simulation, integrated over the external field  $-\infty < H(t) < +\infty$ ). The straight dashed line shows the power-law distribution at the critical point. Notice that fitting power laws to the data would work only very near to  $R_c$ : even with a range of a million in avalanche sizes, the slope has not converged to the asymptotic value. On the other hand, scaling-function predictions (theoretical curves) work well far from the critical point. The inset shows a scaling collapse of the avalanche size distribution (scaled probability versus scaled size), which is used to provide the theoretical curves as described in the text.

Figure 1b presents a simple relationship between earthquake number and magnitude. We expect that there ought to be a simple, underlying reason why earthquakes occur on all different sizes. The properties of very small earthquakes probably depend in detail on the kind of dirt (fault gouge) in the crack. The very largest earthquakes will depend on the geography of the continental plates. But the smooth power-law behaviour indicates that something simpler is happening in between, independent of either the microscopic or the macroscopic details.

There is an analogy here with the behaviour of a fluid. A fluid is very complicated on the microscopic scale, where molecules are bumping into one another: the trajectories of the molecules are chaotic, and depend both on exactly what direction they are moving and what they are made of. However, a simple law describes most fluids on long time and size scales. This law, the Navier–Stokes equation, depends on the constituent molecules only through a few parameters (the density and viscosity). Physics works because simple laws emerge on large scales. In fluids, these microscopic fluctuations and complexities disappear on large scales: for crackling noise, they become scale-invariant and self-similar.

How do we derive the laws for crackling noise? There are two approaches. First, we can calculate analytically the behaviour on long time and size scales by formally coarse-graining over the microscopic fluctuations. This leads us to renormalization-group methods<sup>1–5</sup>, which we discuss in the next section. The analytic approach can be challenging, but it can give useful results and (more important) is the only explanation for why events on all scales should occur. Second, we can make use of universality. If the microscopic details do not matter for the behaviour at long length scales, why not make up a simple model with the same behaviour (in the same universality class) and solve it?

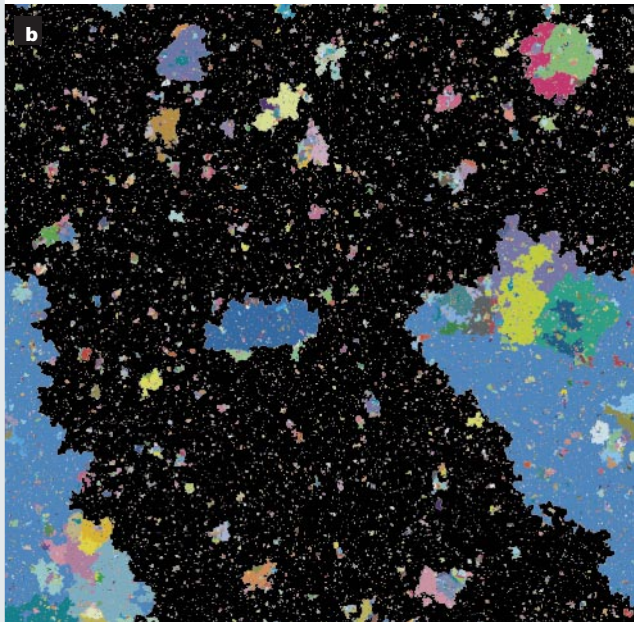
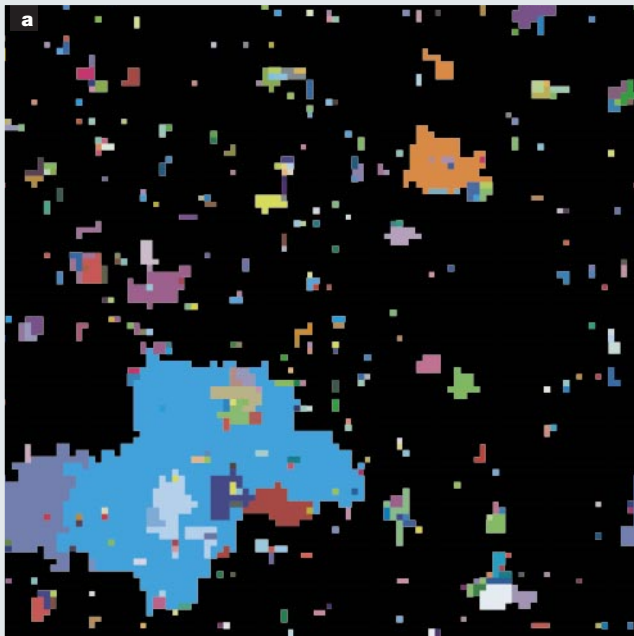


**Figure 3** Self-similarity. Cross-sections of the avalanches during the magnetization of our model<sup>15,73–76</sup>. Here each avalanche is drawn in a separate colour. **a**, A  $100^3$  simulation; **b**, a  $1,000^3$  simulation (a billion domains<sup>74</sup>); both are run at the critical point  $R_c = 2.16$  J where avalanches just barely continue. The black background represents a large avalanche that spans the system: the critical point occurs when avalanches would first span an infinite system.

The model we focus on here is a caricature of a magnetic material<sup>15,46,47,73–77</sup>. A piece of iron will ‘crackle’ as it enters a strong magnetic field, giving what is called Barkhausen noise. We model the iron as a cubic grid of magnetic domains  $S_i$ , whose north pole is either pointing upwards ( $S_i = +1$ ) or downwards ( $S_i = -1$ ). The external field pushes on our domain with a force  $H(t)$ , which will increase with time. Iron can be magnetized because neighbouring domains prefer to point in the same direction: if the six neighbours of our cubic domain are  $S_j$ , then in our model we let their force on our domain be  $\sum_j JS_j$  (where we set the coupling  $J=1$ ). Finally, we model dirt, randomness in the domain shapes, and other kinds of disorder by introducing a random field  $h_i$ , different for each domain and chosen

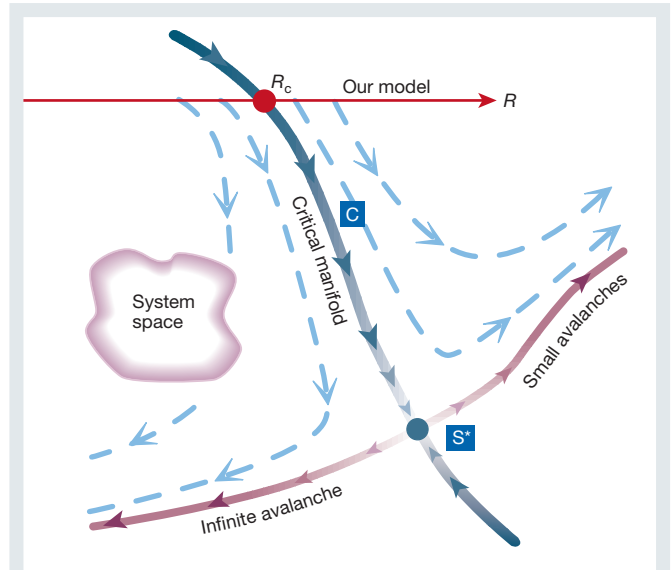


**Figure 4** Renormalization-group flows. The renormalization group is a theory of how coarse-graining to longer length scales introduces a mapping from the space of physical systems to itself. Consider the space of all possible models of magnetic hysteresis. Each model can be coarse-grained, removing some fraction of the microscopic degrees of freedom and introducing more complicated rules so that the remaining ones still flip at the same external fields. This defines a mapping from our space into itself. A fixed point  $S^*$  in this space will be self-similar: because it maps to itself upon coarse-graining, it must have the same behaviour on different length scales. Points that flow into  $S^*$  under coarse-graining share this self-similar behaviour on sufficiently long length scales: they all share the same universality class.

at random from a normal distribution with standard deviation  $R$ , which we call the disorder. The net force on our domain is thus

$$\text{Force on domain } i = H(t) + \sum_j JS_j + h_i \quad (1)$$

The domains in our model all start with their north pole pointing down ( $-1$ ), and flip up as soon as the net force on them becomes positive. This can occur either because  $H(t)$  increases sufficiently (spawning a new avalanche), or because one of their neighbours flipped up, kicking them over (propagating an existing avalanche). (Thermal fluctuations are ignored: a good approximation in many experiments because the domains are large.) If the disorder  $R$  is large, so the  $h_i$  are typically big compared to  $J$ , then most domains flip independently: all the avalanches are small, and we get popping noise. If the disorder is small compared to  $J$ , then typically most of the domains will be triggered by one of their neighbours: one large avalanche will snap up most of our system. In between, we get crackling noise. When the disorder  $R$  is just large enough so that each domain flip on average triggers one of its neighbours (at the critical disorder  $R_c$ ), then we find avalanches on all scales (Figs 2, 3).

What do these avalanches represent? In nonlinear systems with many degrees of freedom, there are often large numbers of metastable states. Local regions in the system can have multiple stable configurations, and many combinations of these local configurations are possible. (A state is metastable when it cannot lower its energy by small rearrangements. It is distinguished from the globally stable state, which is the absolute lowest energy possible for the system.) Avalanches are the rearrangements that occur as our system shifts from one metastable state to another. Our specific interest is in systems with a broad distribution of avalanche sizes, where shifting between metastable states can rearrange anything between a few domains and millions of domains.

There are many choices we made in our model that do not matter at long time and size scales. Because of universality, we can argue<sup>78,79</sup>

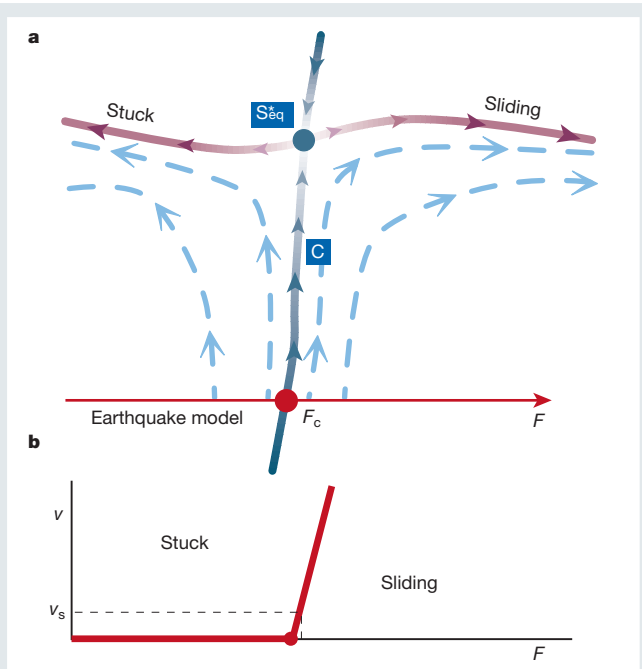


**Figure 5** Flows in the space of earthquake models. A model for earthquakes will have a force  $F$  applied across the front. In models ignoring inertia and velocity-dependent friction<sup>28</sup>, there is a critical force  $F_c$  that just allows the fault to slip forward. **a**, Coarse-graining defines a flow on the space of earthquake models. The fixed point  $S_{eq}^*$  will have a different local flow field from other renormalization-group fixed points, yielding its own universality class of critical exponents and scaling functions. The critical manifold  $C$ , consisting of models that flow into  $S_{eq}^*$ , separates the stuck faults from those that slide forward with an average velocity  $v(F)$ . **b**, The velocity varies with the external force as a power law  $v(F) \sim F^\beta$ . The motion of the continental plates, however, does not fix the force  $F$  across the fault: rather, it sets the average relative velocity to a small value  $v_s$  (centimetres per year). This automatically sets the force across the fault very close to its critical force  $F_c$ . This is one example of self-organized criticality<sup>36,37</sup>.

that the behaviour would be the same if we chose a different grid of domains, or if we changed the distribution of random fields, or if we introduced more realistic random anisotropies and random coupling constants. Were this not the case, we could hardly expect our simple model to explain real experiments.

**The renormalization group and scaling**

To study crackling noise, we use renormalization-group<sup>1-5,78,80</sup> tools developed in the study of second-order phase transitions. The word renormalization has roots in the study of quantum electrodynamics, where the effective charge changes in size (norm) as a function of length scale. The word group refers to the family of coarse-graining operations that are basic to the method: the group product is composition (coarsening repeatedly). The name is unfortunate, however, as the basic coarse-graining operation does not have an inverse, so that the renormalization group does not have the mathematical structure of a group.

The renormalization group studies the way the space of all physical systems maps into itself under coarse-graining (Fig. 4). The coarse-graining operation shrinks the system and removes degrees of freedom on short length scales. Under coarse-graining, we often find a fixed point  $S^*$ : many different models flow into the fixed point and hence share long-wavelength properties. Figure 3 provides a schematic view of coarse-graining: the 1,000<sup>3</sup> cross-section looks (statistically) like the 100<sup>3</sup> section if you blur your eyes by a factor of ten. Much of the mathematical complexity of this field involves finding analytical tools for computing the flow diagram in Fig. 4. Using methods developed to study thermodynamical phase

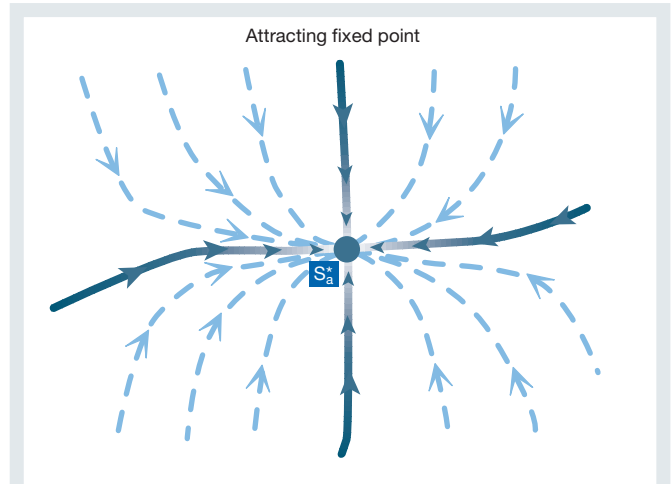


**Figure 6** Attracting fixed point. Often there will be fixed points that attract in all directions. These fixed points describe phases rather than phase transitions. Most phases are rather simple, with fluctuations that die away on long length scales<sup>81</sup>. When fluctuations remain important, they will exhibit self-similarity and power laws called generic scale invariance<sup>83,84</sup>.

transitions<sup>2</sup> and the depinning of charge-density waves<sup>32</sup>, we can calculate for our model the flows for systems in dimensions close to six (the so-called  $\epsilon$ -expansion<sup>78-80</sup>, where  $\epsilon = 6 - d$ , with  $d$  being the dimension of the system). Interpolating between dimensions may seem a surprising thing to do. In our system it gives good predictions even in three dimensions (that is,  $\epsilon = 3$ ), but it is difficult and is not discussed here. Nor will we discuss real-space renormalization-group methods<sup>1</sup> or series-expansion methods. We focus on the relatively simple task of using the renormalization group to justify and explain the universality, self-similarity and scaling observed in nature.

Consider the ‘system space’ for disordered magnets. There is a separate dimension in system space for each possible parameter in a theoretical model (disorder, coupling, next-neighbour coupling, dipolar fields, and so on) or in an experiment (for example, temperature, annealing time and chemical composition). Coarse-graining, however one implements it, gives a mapping from system space into itself: shrinking the system and ignoring the shortest length scales yields a new physical system with identical long-distance physics, but with different (renormalized) values of the parameters. We have abstracted the problem of understanding crackling noise in magnets into understanding a dynamical system acting on a space of dynamical systems.

Figure 4 represents a two-dimensional cross-section of this infinite-dimensional system space. We have chosen the cross-section to include our model (equation (1)): as we vary the disorder  $R$ , our model sweeps out a straight line (red) in system space. The cross-section also includes a fixed point  $S^*$ , which maps into itself under coarse-graining. The system  $S^*$  looks the same on all scales of length and time, because it coarse-grains into itself. We can picture the cross-section of Fig. 4 either as a plane in system space (in which case the arrows and flows depict projections, as in general the real flows will point somewhat out of the plane), or as the curved manifold swept out by our one-parameter model as we coarse-grain (in which case the flows above our model and below the maroon curved line should be ignored).

The flow near  $S^*$  has one unstable direction, leading outwards along the maroon curve (the unstable manifold). In system space, there is a surface of points  $C$  which flow into  $S^*$  under coarse-graining. Because  $S^*$  has only one unstable direction,  $C$  divides system space into two phases. To the left of  $C$ , the systems will have one large, system-spanning avalanche (a snapping noise). To the

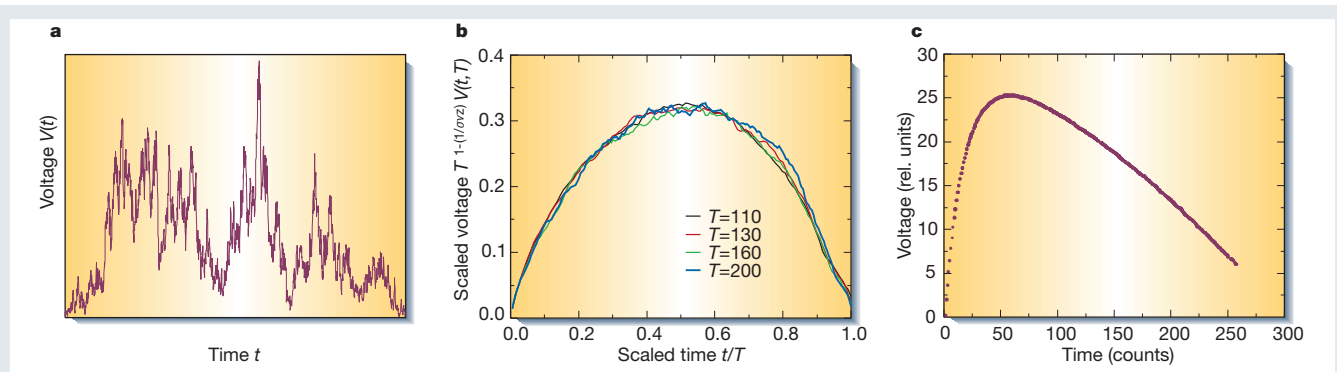


**Figure 7** Scaling of avalanche shapes. **a**, Voltage pulse (number of domains flipped per unit time) during a single large avalanche (arbitrary units). Notice how the avalanche almost stops several times: if the forcing were slightly smaller, this large avalanche would have broken up into two or three smaller ones. The fact that the forcing is just large enough to keep the avalanche growing is the cause of the self-similarity: on average a partial avalanche of size  $S$  will trigger one other of size  $S$ . **b**, Average avalanche shapes<sup>94</sup> for avalanches of different duration for our model (A. Mehta and K.A.D., unpublished results). In addition to predicting power laws,

our theories should describe all behaviour on long scales of length and time (at least in a statistical sense). In particular, by fixing parameters one can predict what are called scaling functions. If we average the voltage as a function of time over all avalanches of a fixed duration, we obtain an average shape. In our simulation, this shape is the same for different durations. **c**, Experimental data of Spasojević *et al.*<sup>95</sup> showing all large avalanches averaged after scaling to fixed duration and area. The experimental average shape is very asymmetric and is not described correctly by our model.

right of **C**, all avalanches are finite and under coarse-graining they all become small (popping noise). As it crosses **C** at the value  $R_c$ , our model goes through a phase transition.

Our model at  $R_c$  is not self-similar on the shortest length scales (where the square lattice of domains still is important), but because it flows into  $S^*$  as we coarse-grain we deduce that it is self-similar on long length scales. Some phase transitions, such as ice melting into water, are abrupt and do not exhibit self-similarity. Continuous phase transitions like ours almost always have self-similar fluctuations on long length scales. In addition, note that our model at  $R_c$  will have the same self-similar structure as  $S^*$  does. Indeed, any experimental or theoretical model lying on the critical surface **C** will share the same long-wavelength critical behaviour. This is the fundamental explanation for universality.

The flows in system space can vary from one class of problems to another: the system space for some earthquake models (Fig. 5a) will have a different flow, and its fixed point will have different scaling behaviour (yielding a different universality class). In some cases, a fixed point will attract all the systems in its vicinity (no unstable directions; Fig. 6). Usually at such attracting fixed points the fluctuations become unimportant at long length scales: the Navier–Stokes equation for fluids described earlier can be viewed as a stable fixed point<sup>81,82</sup>. The coarse-graining process, averaging over many degrees of freedom, naturally smoothens out fluctuations, if they are not amplified near a critical point by the unstable direction. Fluctuations can remain important when a system has random noise in a conserved property, so that fluctuations can die away only by diffusion: in these cases, the whole phase will have self-similar fluctuations, leading to generic scale invariance<sup>83,84</sup>.

Sometimes, even when the system space has an unstable direction as in Fig. 4, the observed behaviour always has avalanches of all scales. This can occur simply because the physical system averages over a range of model parameters (that is, averaging over a range of  $R$  including  $R_c$  in Fig. 4). For example, this can occur by the sweeping of a parameter<sup>85</sup> slowly in time, or varying it gradually in space — either deliberately or through large-scale inhomogeneities.

Self-organized criticality<sup>36,37</sup> can also occur, where the system is controlled so that it sits naturally on the critical surface. Self-organization to the critical point can occur through many mechanisms. In some models of earthquake faults (Fig. 5b), the external force naturally stays near the rupture point because the plates move at a fixed, but very small<sup>20</sup>, velocity with respect to one another (Fig. 5b). (This probably does not occur during large earthquakes, where

inertial effects lead to temporary strain relief<sup>28,86</sup>.) Sandpile models self-organize (if sand is added to the system at an infinitesimal rate) when open boundary conditions<sup>87</sup> are used (which allows sand to leave until the sandpile slope falls to the critical value). Long-range interactions<sup>88–90</sup> between domains can act as a negative feedback in some models, yielding a net external field that remains at the critical point. For each of these cases, once the critical point is understood, adding the mechanism for self-organization is relatively easy.

The case shown in Fig. 4 of ‘plain old criticality’ is what is seen in some<sup>15,73–76</sup> but not all<sup>88–92</sup> models of magnetic materials, in foams<sup>42</sup>, and in some models of earthquakes<sup>28</sup>.

### Beyond power laws

The renormalization group is the theoretical basis for understanding why universality and self-similarity occur. Once we accept that different systems should sometimes share long-distance properties, though, we can quite easily derive some powerful predictions.

To take a tangible example, consider the relation between the duration of an avalanche and its size. In paper crumpling, this is not interesting: all the avalanches seem to be without internal temporal structure<sup>11</sup>. But in magnets, large events take longer to finish, and have an interesting internal statistical self-similarity (Fig. 7a). If we look at all avalanches of a certain duration  $T$  in an experiment, they will have a distribution of sizes  $S$  around some average  $\langle S \rangle_{\text{experiment}}(T)$ . If we look at a theoretical model, it will have a corresponding average size  $\langle S \rangle_{\text{theory}}(T)$ . If our model describes the experiment, these functions must be essentially the same at large  $S$  and large  $T$ . We must allow for the fact that the experimental units of time and size will be different from the ones in the model: the best we can hope for is that  $\langle S \rangle_{\text{experiment}}(T) = A \langle S \rangle_{\text{theory}}(T/B)$ , for some rescaling factors  $A$  and  $B$ .

Now, instead of comparing our model to experiment, we can compare it to itself on a slightly larger timescale<sup>93</sup>. If the timescale is expanded by a small factor  $B = 1/(1 - \delta)$ , then the rescaling of the size will also be small, say  $1 + a\delta$ . Now

$$\langle S \rangle(T) = (1 + a\delta) \langle S \rangle((1 - \delta)T) \tag{2}$$

Making  $\delta$  very small yields the simple relation  $a \langle S \rangle = T d \langle S \rangle / dT$ , which can be solved to give the power-law relation  $\langle S \rangle(T) = S_0 T^a$ . The exponent  $a$  is called a critical exponent, and is a universal prediction of a given theory. (This means that if the theory correctly describes an experiment, the critical exponents will agree.) In our

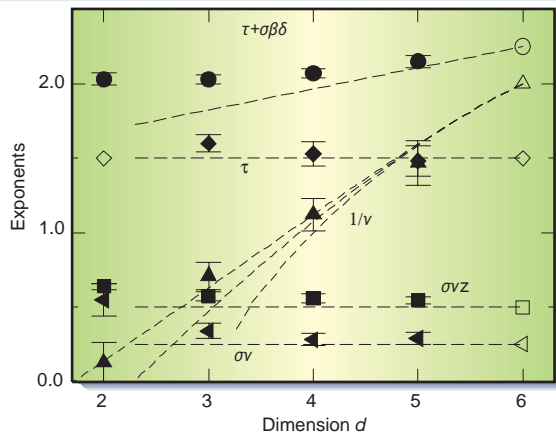


**Figure 8** Critical exponents in various dimensions. We test our  $\epsilon$ -expansion predictions<sup>78,80</sup> by measuring<sup>76</sup> the various critical exponents numerically in up to five spatial dimensions. The various exponents are described in the text. All exponents are calculated only to linear order in  $\epsilon$ , except for the correlation length exponent  $\nu$ , where we use results from other models<sup>78,80</sup>. The agreement even in three dimensions is remarkably good, considering that we are expanding in  $\epsilon$  where  $\epsilon = 3$ . Note that perturbing in dimension for our system is not only complicated, but also controversial<sup>111</sup> (see also section VI.C of ref. 78 and section V of ref. 76).

work, we write the exponent  $a$  relating time to size in terms of three other critical exponents,  $a = 1/\sigma\nu$ .

There are several basic critical exponents, which arise in various combinations depending on the physical property being studied. The details of the naming and relationships between these exponents are not a focus of this article. Briefly, the cutoff in the avalanche size distribution in Fig. 2 gets larger as one approaches the critical disorder as  $(R - R_c)^{-1/\sigma}$  (Fig. 2). The typical length  $L$  of the largest avalanche is proportional to  $(R - R_c)^{-\nu}$ . At  $R_c$ , the probability of having an avalanche of size  $S$  is  $S^{-(\tau + \alpha\beta\delta)}$  (Fig. 2); and just at the critical field it is  $S^{-\tau}$ . (Note that the small change in scale  $\delta$  should not be confused with the critical exponent  $\delta$ .) The fractal dimension of the avalanches is  $1/\sigma\nu$ , meaning the spatial extent  $L$  of an avalanche is proportional to the size  $S^{\sigma\nu}$ . The duration  $T$  of an avalanche of spatial extent  $L$  is  $L^z$ .

To specialists in critical phenomena, these exponents are central; whole conversations will seem to rotate around various combinations of Greek letters. Critical exponents are one of the relatively easy parameters to calculate from the various analytic approaches, and so have attracted the most attention. They are derived from the eigenvalues of the linearized flows about the fixed point  $S^*$  in Fig. 4. Figure 8 shows our numerical estimates<sup>76</sup> for several critical exponents in our model in various spatial dimensions, together with our  $6-\epsilon$  expansions<sup>78,80</sup> for them. Of course the key challenge is not to get analytical work to agree with numerics: it is to get theory to agree with experiment. Figure 9 shows that our model does well in describing a wide variety of experiments, but that two alternative models (with different flows around their fixed points) also fit.

Critical exponents are not everything; many other scaling predictions, explaining wide varieties of behaviour, are relatively straightforward to extract from numerical simulations. Universality extends even to those properties of long length scales for which written formulas do not yet exist. Perhaps the most important of these other predictions are the universal scaling functions. For example, consider the time history of the avalanches,  $V(t)$ , denoting the number of domains flipping per unit time. (We call it  $V$  because it is usually measured as a voltage in a pickup coil.) Each avalanche has large fluctuations, but we can average over many avalanches to get a typical shape. Figure 7b shows the average over all avalanches of fixed duration  $T$ , which we shall call  $\langle V \rangle(T, t)$ . Universality again suggests that this average should be the same for experiment and a successful

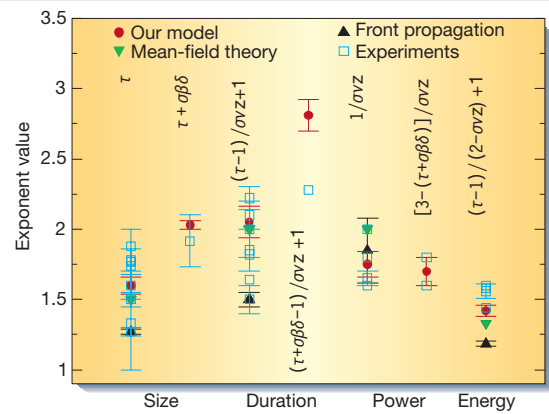


**Figure 9** Comparing experiments with theory: critical exponents. Different experiments on crackling noise in magnets measure different combinations of the universal critical exponents. Here we compare experimental measurements<sup>88,95,112–122</sup> (see also Table I of ref. 73) to the theoretical predictions for three models: our model<sup>15,73–76</sup>, the front-propagation model<sup>46–51,121</sup> and mean-field theory. (In mean-field theory our coupling  $J$  in equation (1) couples all pairs of spins: such long-range interactions occur because of the boundaries in models with magnetic dipolar forces<sup>90</sup>. Mean-field theory is equivalent to a successful model with a single degree of freedom<sup>123,124</sup>.) Shown are power laws that give the probability of obtaining an avalanche of a given size, duration or energy at the critical point; also shown is the critical exponent giving the power as a function of frequency<sup>94</sup> (due to the internal structure of the avalanches; Fig. 7a). In each pair of columns, the first column includes only avalanches at external fields  $H$  in equation (1) where the largest avalanches occur, and the second column (when it exists) includes all avalanches. The various combinations of the basic critical exponents can be derived from exponent equality calculations similar to the one discussed in the text<sup>73,80,94</sup>. Many of the experiments were done years before the theories were developed, and many did not report error bars. All three theories do well (especially considering the possible systematic errors in fitting power laws to the experimental measurements; see Fig. 2). Recent work indicates a clumping of experimental values around the mean-field and front-propagation predictions<sup>121</sup>.

theory, apart from an overall shift in time and voltage scales:  $\langle V \rangle_{\text{experiment}}(T, t) = A \langle V \rangle_{\text{theory}}(T/B, t/B)$ . Comparing our model to itself with a shifted timescale becomes straightforward if we change variables: let  $\nu(T, t/T) = \langle V \rangle(T, t)$ , so  $\nu(T, t/T) = A\nu(T/B, t/T)$ . Here  $t/T$  is a particularly simple example of a scaling variable. Now, if we rescale time by a small factor  $B = 1/(1 - \delta)$ , we have  $\nu(T, t/T) = (1 + b\delta)\nu(t/T, (1 - \delta)T)$ . Again, making  $\delta$  small we find  $b\nu = T\partial\nu/\partial T$ , with solution  $\nu = \nu_0 T^b$ . However, the integration constant  $\nu_0$  will now depend on  $t/T$ ,  $\nu_0 = V(t/T)$ , so we arrive at the scaling form

$$\langle V \rangle(t, T) = T^b \mathbf{V}(t/T) \tag{3}$$

where the entire scaling function  $\mathbf{V}$  is a universal prediction of the theory.

Figure 7b,c shows the universal scaling functions  $\mathbf{V}$  for our model<sup>94</sup> and an experiment<sup>95</sup>. For our model, we have drawn what are called scaling collapses, a simple but powerful way both to check that we are in the scaling regime, and to measure the universal scaling function. Using the form of the scaling equation (3), we simply plot  $T^{-b} \langle V \rangle(t, T)$  versus  $t/T$ , for a series of long times  $T$ . All the plots fall onto the same curve, (which means that our avalanches are large enough to be self-similar. (If in the scaling collapse the corresponding plots do not all look alike, then any power laws measured are probably accidental.) The scaling collapse also provides us with a numerical evaluation of the scaling function  $\mathbf{V}$ . Note that we use  $1/\sigma\nu - 1$  for the critical exponent  $b$ . This is an example of an

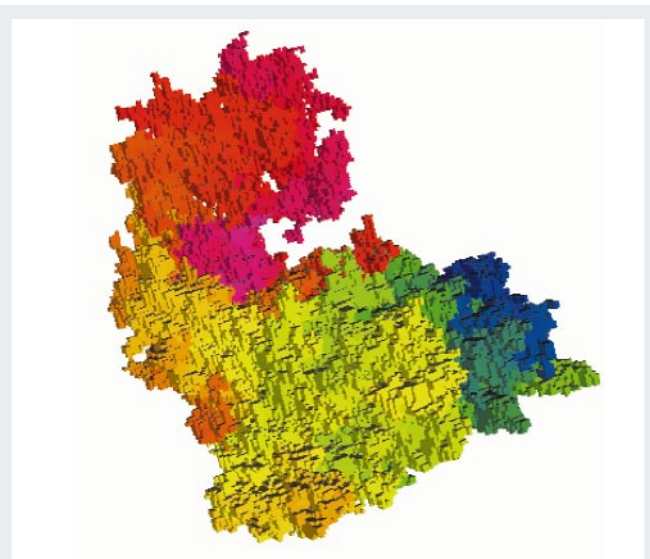


**Figure 10** Fractal spatial structure of an avalanche<sup>74</sup>. Fractal structures, as well as power laws, are characteristic of systems at their critical point. This moderate-sized avalanche involved the flipping of 282,785 domains in our simulation. The colours represent time: the first domains to flip are coloured blue, and the last pink. So far, there have not been many experiments showing the spatial structure of avalanches<sup>125</sup>. When experiments become available, there are a wealth of predictions of the scaling theories that we could test. Other systems<sup>28,55,126</sup> display a qualitatively different kind of avalanche spatial structure, where the avalanche is made up of many small disconnected pieces, which trigger one another through the waves emitted as they flip.

exponent equality and is easily derived from the fact that  $\langle S \rangle(T) = \int \langle V \rangle(t, T) dt = \int T^b \mathbf{V}(t/T) dt \sim T^{b+1}$ , and the scaling relation  $\langle S \rangle(T) \sim T^{1/\sigma_V}$ .

Notice that our model and the experiment have different shapes for  $\mathbf{V}$ . The other two models from Fig. 9 also give much more symmetrical forms for  $\mathbf{V}$  than the experiment does<sup>94</sup>. How do we react to this? Our models are falsified if any of the predictions are shown to be wrong asymptotically on long scales of length and time. If duplication of this measurement by other groups continues to show this asymmetry, then our theory is obviously incomplete. Even if later experiments in other systems agree with our predictions, it would seem that this particular system is described by an undiscovered universality class. Incorporating insights from careful experiments to refine the theoretical models has always been crucial in the broad field of critical phenomena. The message we emphasize here is that scaling functions can provide a sharper tool for discriminating between different universality classes than critical exponents.

In broad terms, most common properties that involve large scales of length and time have scaling forms. Using self-similarity, we can write functions of  $N$  variables in terms of scaling functions of  $N-1$  variables:  $F(x, y, z) = z^{-\alpha} \mathbf{F}(x/z^\beta, y/z^\gamma)$ . In the inset to Fig. 2, we show the scaling collapse for the avalanche size distribution:  $D(S, R) = S^{-(\tau + \sigma\beta)} \mathbf{D}((R - R_c)/S^{-\sigma})$ . (This example illustrates that scaling works not only at  $R_c$  but also near  $R_c$ ; the maroon unstable manifold in Fig. 4 governs the behaviour for systems near the critical manifold C.)

Many other kinds of properties beyond critical exponents and scaling functions can be predicted from these theories. Figure 10 shows the spatial structure of a large avalanche in our model: notice that not only is it fractal (rugged on all scales), but also that it is longer than it is wide<sup>96</sup>, and that it is topologically interesting<sup>97</sup>. (It has tunnels, and sometimes during the avalanche it forms a tunnel and later winds itself through it, forming a knot. It is interesting that the topology of the interfaces in the three-dimensional Ising model have

applications in quantum gravity<sup>97</sup>.) In other systems, the statistics of all of these properties have been shown to be universal on long scales of length and time.

### Continuing challenges

Despite recent developments, our understanding of crackling noise is far from complete. There are only a few systems<sup>28,32,48,49,53,54,78-80</sup> where the renormalization-group framework has substantially explained even the behaviour of the numerical models. There are several other approaches<sup>63,64,87,98-100</sup> that have been developed to study crackling noise, many of which share our view of developing effective descriptions on long scales of length and time. But the successes remain dwarfed by the bewildering variety of systems that crackle. Achieving a global perspective on the universality classes for crackling noise remains an open challenge.

An even more important challenge is to make quantitative comparison between the theoretical models and experimental systems. We believe that going beyond power laws will be crucial in this endeavour. The past focus on critical exponents has sometimes been frustrating: it is too easy to find power laws over limited scaling ranges<sup>101</sup>, and too easy to find models which roughly fit them. It also seems unfulfilling, summarizing a complex morphology into a single critical exponent. We believe that measuring a power law is almost never definitive by itself: a power law in conjunction with evidence that the morphology is scale invariant (for example, a scaling collapse) is crucial. By aggressively pursuing quantitative comparisons of other, richer measures of morphology such as the universal scaling functions, we will be better able both to discriminate among theories and to ensure that a measured power law corresponds to a genuine scaling behaviour.

Another challenge is to start thinking about the key ways that these complex spatiotemporal systems differ from the phase transitions we understand from equilibrium critical behaviour. (The renormalization-group tools developed by our predecessors are seductively illuminating, and it is always easy to focus where the light is good.) For example, in several of these systems there are collective, dynamical ‘memory’ effects<sup>15,102-105</sup> that may even have practical applications<sup>106</sup>. The quest for a scaling theory of crackling phenomena needs to be viewed as part of the larger process of understanding the dynamics of these nonlinear, non-equilibrium systems.

A final challenge is to make the study of crackling noise profitable. Less noise from candy wrappers<sup>11-13</sup> in cinemas and theatres is not the most pressing of global concerns. Making money from fluctuations in stock prices is already big business<sup>58,59</sup>. Predicting earthquakes over the short term probably will not be feasible using these approaches<sup>107</sup>, but longer-term prediction of impending large earthquakes may be both possible<sup>86</sup> and useful (for example, for guiding local building codes). Understanding that the large-scale behaviour relies on only a few emergent material parameters (disorder and external field for our model of magnetism) will lead to the study of how these parameters depend on the microphysics. We might dream, for example, of learning eventually how to shift an active earthquake fault into a harmless, continuously sliding regime by adding lubricants to the fault gouge. In the meantime, crackling noise is basic research at its elegant, fundamental best. □

1. Kadanoff, L. P. Scaling laws for Ising models near  $T_c$ . *Physics* **2**, 263–272 (1966).
2. Wilson, K. G. Problems in physics with many scales of length. *Sci. Am.* **241**, 140–157 (1979).
3. Pfeuty, P. & Toulouse, G. *Introduction to the Renormalization Group and to Critical Phenomena* (Wiley, London, 1977).
4. Yeomans, J. M. *Statistical Mechanics of Phase Transitions* (Oxford Univ. Press, Oxford, 1992).
5. Fisher, M. E. Renormalization group theory: its basis and formulation in statistical physics. *Rev. Mod. Phys.* **70**, 653–681 (1998).
6. Martin, P. C., Siggia, E. D. & Rose, H. A. Statistical dynamics of classical systems. *Phys. Rev. A* **8**, 423–437 (1973).
7. De Dominicis, C. Dynamics as a substitute for replicas in systems with quenched random impurities. *Phys. Rev. B* **18**, 4913–4919 (1978).
8. Sompolinsky, H. & Zippelius, A. Relaxational dynamics of the Edwards-Anderson model and the mean-field theory of spin-glasses. *Phys. Rev. B* **25**, 6860–6875 (1982).
9. Zippelius, A. Critical-dynamics of spin-glasses. *Phys. Rev. B* **29**, 2717–2723 (1984).
10. Gutenberg, B. & Richter, C. F. *Seismicity of the Earth and Associated Phenomena* (Princeton Univ.

- Press, Princeton, 1954).
11. Houle, P. A. & Sethna, J. P. Acoustic emission from crumpling paper. *Phys. Rev. E* **54**, 278–283 (1996).
  12. Kramer, E. M. & Lobkovsky, A. E. Universal power law in the noise from a crumpled elastic sheet. *Phys. Rev. E* **53**, 1465–1469 (1996).
  13. Glanz, J. No hope of silencing the phantom crinklers of the opera. *New York Times* 1 June 2000, A14 (2000).
  14. Sethna, J. P. Hysteresis and avalanches <<http://www.lassp.cornell.edu/sethna/hysteresis/hysteresis.html>> (1996).
  15. Sethna, J. P. *et al.* Hysteresis and hierarchies: dynamics of disorder-driven first-order phase transformations. *Phys. Rev. Lett.* **70**, 3347–3351 (1993).
  16. Burridge, R. & Knopoff, L. Model and theoretical seismicity. *Bull. Seismol. Soc. Am.* **57**, 3411–3471 (1967).
  17. Rice, J. R. & Ruina, A. L. Stability of steady frictional slipping. *J. Appl. Mech.* **50**, 343 (1983).
  18. Carlson, J. M. & Langer, J. S. Mechanical model of an earthquake fault. *Phys. Rev. A* **40**, 6470–6484 (1989).
  19. Bak, P. & Tang, C. Earthquakes as a self-organized critical phenomenon. *J. Geophys. Res.* **94**, 15635–15637 (1989).
  20. Chen, K., Bak, P. & Obukhov, S. P. Self-organized criticality in a crack-propagation model of earthquakes. *Phys. Rev. A* **43**, 625–630 (1991).
  21. Olami, Z., Feder, H. J. S. & Christensen, K. Self-organized criticality in a continuous, nonconservative cellular automaton modeling earthquakes. *Phys. Rev. Lett.* **68**, 1244–1247 (1992).
  22. Miltenberger, P., Sornette, D. & Vanette, C. Fault self-organization and optimal random paths selected by critical spatiotemporal dynamics of earthquakes. *Phys. Rev. Lett.* **71**, 3604–3607 (1993).
  23. Crowie, P. A., Vanette, C. & Sornette, D. Statistical physics model for the spatiotemporal evolution of faults. *J. Geophys. Res. Solid Earth* **98**, 21809–21821 (1993).
  24. Carlson, J. M., Langer, J. S. & Shaw, B. E. Dynamics of earthquake faults. *Rev. Mod. Phys.* **66**, 657–670 (1994).
  25. Myers, C. R., Shaw, B. E. & Langer, J. S. Slip complexity in a crustal-plane model of an earthquake fault. *Phys. Rev. Lett.* **77**, 972–975 (1996).
  26. Shaw, B. E. & Rice, J. R. Existence of continuum complexity in the elastodynamics of repeated fault ruptures. *J. Geophys. Res.* **105**, 23791–23810 (2000).
  27. Ben-Zion, Y. & Rice, J. R. Slip patterns and earthquake populations along different classes of faults in elastic solids. *J. Geophys. Res.* **100**, 12959–12983 (1995).
  28. Fisher, D. S., Dahmen, K., Ramanathan, S. & Ben-Zion, Y. Statistics of earthquakes in simple models of heterogeneous faults. *Phys. Rev. Lett.* **78**, 4885–4888 (1997).
  29. Fisher, D. S. Threshold behavior of charge-density waves pinned by impurities. *Phys. Rev. Lett.* **50**, 1486–1489 (1983).
  30. Fisher, D. S. Sliding charge-density waves as a dynamic critical phenomenon. *Phys. Rev. B* **31**, 1396–1427 (1985).
  31. Littlewood, P. B. Sliding charge-density waves: a numerical study. *Phys. Rev. B* **33**, 6694–6708 (1986).
  32. Narayan, O. & Fisher, D. S. Critical behavior of sliding charge-density waves in 4- $\epsilon$  dimensions. *Phys. Rev. B* **46**, 11520–11549 (1992).
  33. Middleton, A. A. & Fisher, D. S. Critical behavior of charge-density waves below threshold: numerical and scaling analysis. *Phys. Rev. B* **47**, 3530–3552 (1993).
  34. Myers, C. R. & Sethna, J. P. Collective dynamics in a model of sliding charge-density waves. I. Critical behavior. *Phys. Rev. B* **47**, 11171–11192 (1993).
  35. Thorne, R. E. Charge-density-wave conductors. *Phys. Today* **49**, 42–47 (1996).
  36. Bak, P., Tang, C. & Wiesenfeld, K. Self-organized criticality: an explanation for 1/f noise. *Phys. Rev. Lett.* **59**, 381–384 (1987).
  37. Bak, P., Tang, C. & Wiesenfeld, K. Self-organized criticality. *Phys. Rev. A* **38**, 364–374 (1988).
  38. deGennes, P. G. *Superconductivity of Metals and Alloys* p. 83 (Benjamin, New York, 1966).
  39. Feynman, R. P., Leighton, R. B. & Sands, M. *The Feynman Lectures on Physics* Vol. II Sect. 37–3 (Addison Wesley, Reading, MA, 1963–1965).
  40. Jaeger, H. M., Liu, C. & Nagel, S. R. Relaxation at the angle of repose. *Phys. Rev. Lett.* **62**, 40–43 (1989).
  41. Nagel, S. R. Instabilities in a sandpile. *Rev. Mod. Phys.* **64**, 321–325 (1992).
  42. Tewari, S. *et al.* Statistics of shear-induced rearrangements in a two-dimensional model foam. *Phys. Rev. E* **60**, 4385–4396 (1999).
  43. Solé, R. V. & Manrubia, S. C. Extinction and self-organized criticality in a model of large-scale evolution. *Phys. Rev. E* **54**, R42–R45 (1996).
  44. Newman, M. E. J. Self-organized criticality, evolution, and the fossil extinction record. *Proc. R. Soc. Lond. B* **263**, 1605–1610 (1996).
  45. Newman, M. E. J. & Palmer, R. G. Models of extinction: a review. Preprint <http://xxx.lanl.gov> (1999).
  46. Cieplak, M. & Robbins, M. O. Dynamical transition in quasistatic fluid invasion in porous media. *Phys. Rev. Lett.* **60**, 2042–2045 (1988).
  47. Koiller, B. & Robbins, M. O. Morphology transitions in three-dimensional domain growth with Gaussian random fields. *Phys. Rev. B* **62**, 5771–5778 (2000).
  48. Nattermann, T., Stepanow, S., Tang, L. H. & Leschhorn, N. Dynamics of interface depinning in a disordered medium. *J. Phys. II (Paris)* **2**, 1483–1488 (1992).
  49. Narayan, O. & Fisher, D. S. Threshold critical dynamics of driven interfaces in random media. *Phys. Rev. B* **48**, 7030–7042 (1993).
  50. Leschhorn, H., Nattermann, T., Stepanow, S. & Tang, L.-H. Driven interface depinning in a disordered medium. *Ann. Phys. (Leipzig)* **6**, 1–34 (1997).
  51. Roters, L., Hucht, A., Lubck, S., Nowak, U. & Usadel, K. D. Depinning transition and thermal fluctuations in the random-field Ising model. *Phys. Rev. E* **60**, 5202–5207 (1999).
  52. Field, S., Witt, J., Nori, F. & Ling, X. Superconducting vortex avalanches. *Phys. Rev. Lett.* **74**, 1206–1209 (1995).
  53. Ertas, D. & Kardar, M. Anisotropic scaling in depinning of a flux line. *Phys. Rev. Lett.* **73**, 1703–1706 (1994).
  54. Ertas, D. & Kardar, M. Anisotropic scaling in threshold critical dynamics of driven directed lines. *Phys. Rev. B* **53**, 3520–3542 (1996).
  55. Lilly, M. P., Wootters, A. H. & Hallock, R. B. Spatially extended avalanches in a hysteretic capillary condensation system: superfluid He-4 in nuclepore. *Phys. Rev. Lett.* **77**, 4222–4225 (1996).
  56. Guyer, R. A. & McCall, K. R. Capillary condensation, invasion percolation, hysteresis, and discrete memory. *Phys. Rev. B* **54**, 18–21 (1996).
  57. Ortín, J. *et al.* Experiments and models of avalanches in martensites. *J. Phys. IV (Paris)* **5**, 209–214 (1995).
  58. Bouchaud, J. P. Power-laws in economy and finance: some ideas from physics. (Proc. Santa Fe Conf. Beyond Efficiency.) *J. Quant. Finance* (in the press); also available as preprint [cond-mat/0008103](http://xxx.lanl.gov) at <<http://xxx.lanl.gov>>.
  59. Bak, P., Paczuski, M. & Shubik, M. Price variations in a stock market with many agents. *Physica A* **246**, 430–453 (1997).
  60. Lu, E. T., Hamilton, R. J., McTiernan, J. M. & Bromond, K. R. Solar flares and avalanches in driven dissipative systems. *Astrophys. J.* **412**, 841–852 (1993).
  61. Carreras, B. A., Newman, D. E., Dobson, I. & Poole, A. B. Initial evidence for self-organized criticality in electrical power system blackouts. In *Proc. 33rd Hawaii Int. Conf. Syst. Sci.* (ed. Sprague, R. H. Jr) (IEEE Comp. Soc., Los Alamitos, CA, 2000).
  62. Sachtjen, M. L., Carreras, B. A. & Lynch, V. E. Disturbances in a power transmission system. *Phys. Rev. E* **61**, 4877–4882 (2000).
  63. Carlson, J. M. & Doyle, J. Highly optimized tolerance: a mechanism for power laws in designed systems. *Phys. Rev. E* **60**, 1412–1427 (1999).
  64. Carlson, J. M. & Doyle, J. Highly optimized tolerance: robustness and design in complex systems. *Phys. Rev. Lett.* **84**, 2529–2532 (2000).
  65. Newman, M. The power of design. *Nature* **405**, 412–413 (2000).
  66. Galam, S. Rational group decision making: a random field Ising model at  $T=0$ . *Physica A* **238**, 66–80 (1997).
  67. Petri, A., Paparo, G., Vespignani, A., Alippi, A. & Costantini, M. Experimental evidence for critical dynamics in microfracturing processes. *Phys. Rev. Lett.* **73**, 3423–3426 (1994).
  68. Garcimartin, A., Guarino, A., Bellon, L. & Ciliberto, S. Statistical properties of fracture precursors. *Phys. Rev. Lett.* **79**, 3202–3205 (1997).
  69. Curtin, W. A. & Scher, H. Analytic model for scaling of breakdown. *Phys. Rev. Lett.* **67**, 2457–2460 (1991).
  70. Herrman, H. J. & Roux, S. (eds) *Statistical Models for the Fracture of Disordered Media* (North Holland, Amsterdam, 1990).
  71. Chakrabarti, B. K. & Benguigui, L. G. *Statistical Physics of Fracture and Breakdown in Disordered Systems* (Clarendon, Oxford, 1997).
  72. Zapperi, S., Ray, P., Stanley, H. E. & Vespignani, A. First-order transition in the breakdown of disordered media. *Phys. Rev. Lett.* **78**, 1408–1411 (1997).
  73. Perković, O., Dahmen, K. A. & Sethna, J. P. Avalanches, Barkhausen noise, and plain old criticality. *Phys. Rev. Lett.* **75**, 4528–4531 (1995).
  74. Kuntz, M. C., Perković, O., Dahmen, K. A., Roberts, B. W. & Sethna, J. P. Hysteresis, avalanches, and noise: numerical methods. *Comput. Sci. Eng.* **1**, 73–81 (1999).
  75. Kuntz, M. C. & Sethna, J. P. Hysteresis, avalanches, and noise: numerical methods <<http://www.lassp.cornell.edu/sethna/hysteresis/code/>> (1998).
  76. Perković, O., Dahmen, K. A. & Sethna, J. P. Disorder-induced critical phenomena in hysteresis: numerical scaling in three and higher dimensions. *Phys. Rev. B* **59**, 6106–6119 (1999).
  77. Berger, A., Inomata, A., Jiang, J. S., Pearson, J. E. & Bader, S. D. Experimental observation of disorder-driven hysteresis-loop criticality. *Phys. Rev. Lett.* **85**, 4176–4179 (2000).
  78. Dahmen, K. A. & Sethna, J. P. Hysteresis, avalanches, and disorder induced critical scaling: a renormalization group approach. *Phys. Rev. B* **53**, 14872–14905 (1996).
  79. da Silva, R. & Kardar, M. Critical hysteresis for N-component magnets. *Phys. Rev. E* **59**, 1355–1367 (1999).
  80. Dahmen, K. A. & Sethna, J. P. Hysteresis loop critical exponents in 6- $\epsilon$  dimensions. *Phys. Rev. Lett.* **71**, 3222–3225 (1993).
  81. Visscher, P. B. Renormalization-group derivation of Navier-Stokes equation. *J. Stat. Phys.* **38**, 989–1013 (1985).
  82. Kadanoff, L. P., McNamara, G. R. & Zanetti, G. From automata to fluid flow: comparisons of simulation and theory. *Phys. Rev. A* **40**, 4527–4541 (1989).
  83. Hwa, T. & Kardar, M. Dissipative transport in open systems: an investigation of self-organized criticality. *Phys. Rev. Lett.* **62**, 1813–1816 (1989).
  84. Grinstein, G., Lee, D.-H. & Sachdev, S. Conservation laws, anisotropy, and “self-organized criticality” in noisy non-equilibrium systems. *Phys. Rev. Lett.* **64**, 1927–1930 (1990).
  85. Sornette, D. Sweeping of an instability—an alternative to self-organized criticality to get power laws without parameter tuning. *J. Phys. I (Paris)* **4**, 209–221 (1994).
  86. Sykes, L. R., Shaw, B. E. & Scholz, C. H. Rethinking earthquake prediction. *Pure Appl. Geophys.* **155**, 207 (1999).
  87. Carlson, J. M., Chayes, J. T., Grannan, E. R. & Swindle, G. H. Self-organized criticality and singular diffusion. *Phys. Rev. Lett.* **65**, 2547–2550 (1990).
  88. Urbach, J. S., Madison, R. C. & Markert, J. T. Interface depinning, self-organized criticality, and the Barkhausen effect. *Phys. Rev. Lett.* **75**, 276–279 (1995).
  89. Narayan, O. Self-similar Barkhausen noise in magnetic domain wall motion. *Phys. Rev. Lett.* **77**, 3855–3857 (1996).
  90. Zapperi, P., Cizeau, P., Durin, G. & Stanley, H. E. Dynamics of a ferromagnetic domain wall: avalanches, depinning transition, and the Barkhausen effect. *Phys. Rev. B* **58**, 6353–6366 (1998).
  91. Pazmandi, F., Zarand, G. & Zimanyi, G. T. Self-organized criticality in the hysteresis of the Sherrington-Kirkpatrick model. *Phys. Rev. Lett.* **83**, 1034–1037 (1999).
  92. Pazmandi, F., Zarand, G. & Zimanyi, G. T. Self-organized criticality in the hysteresis of the Sherrington-Kirkpatrick model. *Physica B* **275**, 207–211 (2000).
  93. Perković, O., Dahmen, K. A. & Sethna, J. P. Disorder-induced critical phenomena in hysteresis: a numerical scaling analysis. Preprint [cond-mat/9609072](http://xxx.lanl.gov), appendix A, at <<http://xxx.lanl.gov>> (1996).
  94. Kuntz, M. C. & Sethna, J. P. Noise in disordered systems: the power spectrum and dynamic exponents in avalanche models. *Phys. Rev. B* **62**, 11699–11708 (2000).
  95. Spasojević, D., Bukvić, S., Milošević, S. & Stanley, H. E. Barkhausen noise: elementary signals, power laws, and scaling relations. *Phys. Rev. E* **54**, 2531–2546 (1996).
  96. Family, F., Vicsek, T. & Meakin, P. Are random fractal clusters isotropic? *Phys. Rev. Lett.* **55**, 641–644 (1985).
  97. Dotsenko, V. S. *et al.* Critical and topological properties of cluster boundaries in the 3D Ising model. *Phys. Rev. Lett.* **71**, 811–814 (1993).
  98. Kadanoff, L. P., Nagel, S. R., Wu, L. & Zhou, S.-M. Scaling and universality in avalanches. *Phys. Rev. A* **39**, 6524–6537 (1989).
  99. Dhar, D. The Abelian sandpile and related models. *Physica A* **263**, 4–25 (1999).
  100. Paczuski, M., Maslov, S. & Bak, P. Avalanche dynamics in evolution, growth, and depinning models. *Phys. Rev. E* **414**–443 (1996).
  101. Malcai, O., Lidar, D. A., Biham, O. & Avnir, D. Scaling range and cutoffs in empirical fractals. *Phys. Rev. E* **56**, 2817–2828 (1997).
  102. Fleming, R. M. & Schneemeyer, L. F. Observation of a pulse-duration memory effect in  $K_{0.30}MoO_3$ . *Phys. Rev. Lett.* **33**, 2930–2932 (1986).

103. Coppersmith, S. N. & Littlewood, P. B. Pulse-duration memory effect and deformable charge-density waves. *Phys. Rev. B* **36**, 311–317 (1987).
104. Middleton, A. A. Asymptotic uniqueness of the sliding state for charge-density waves. *Phys. Rev. Lett.* **68**, 670–673 (1992).
105. Amengual, A. *et al.* Systematic study of the martensitic transformation in a Cu-Zn-Al alloy—reversibility versus irreversibility via acoustic emission. *Thermochim. Acta* **116**, 195–308 (1987).
106. Perković, O. & Sethna, J. P. Improved magnetic information storage using return-point memory. *J. Appl. Phys.* **81**, 1590–1597 (1997).
107. Pepke, S. L., Carlson, J. M. & Shaw, B. E. Prediction of large events on a dynamical model of a fault. *J. Geophys. Res.* **99**, 6769 (1994).
108. Council of the National Seismic System. Composite Earthquake Catalog Archive <<http://www.cnss.org>> (2000).
109. US Geological Survey National Earthquake Information Center. Earthquake information for the world <<http://www.neic.cr.usgs.gov>> (2001).
110. Sethna, J. P., Kuntz, M. C., & Houle, P. A. Crackling noise <<http://simscience.org/crackling>>. (1999).
111. Brézin E. & De Dominicis C. Dynamics versus replicas in the random field Ising model. *C.R. Acad. Sci. II* **327**, 383–390 (1999).
112. Cote, P. J. & Meisel, L. V. Self-organized criticality and the Barkhausen effect. *Phys. Rev. Lett.* **67**, 1334–1337 (1991).
113. Meisel, L. V. & Cote, P. J. Power laws, flicker noise, and the Barkhausen effect. *Phys. Rev. B* **46**, 10822–10828 (1992).
114. Stierstadt, K. & Boeckh, W. Die Temperaturabhängigkeit des Magnetischen Barkhauseneffekts. 3. Die Sprunggrößenverteilung längs der Magnetisierungskurve. *Z. Phys.* **186**, 154 (1965).
115. Bertotti, G., Durin, G. & Magni, A. Scaling aspects of domain wall dynamics and Barkhausen effect in ferromagnetic materials. *J. Appl. Phys.* **75**, 5490–5492 (1994).
116. Bertotti, G., Fiorillo, F. & Montorsi, A. The role of grain size in the magnetization process of soft magnetic materials. *J. Appl. Phys.* **67**, 5574–5576 (1990).
117. Lieneweg, U. Barkhausen noise of 3% Si-Fe strips after plastic deformation. *IEEE Trans. Magn.* **10**, 118–120 (1974).
118. Lieneweg, U. & Grosse-Nobis, W. Distribution of size and duration of Barkhausen pulses and energy spectrum of Barkhausen noise investigated on 81% nickel-iron after heat treatment. *Int. J. Magn.* **3**, 11–16 (1972).
119. Bittel, H. Noise of ferromagnetic materials. *IEEE Trans. Magn.* **5**, 359–365 (1969).
120. Montalenti, G. Barkhausen noise in ferromagnetic materials. *Z. Angew. Phys.* **28**, 295–300 (1970).
121. Durin, G. & Zapperi, S. Scaling exponents for Barkhausen avalanches in polycrystalline and amorphous ferromagnets. *Phys. Rev. Lett.* **84**, 4705–4708 (2000).
122. Petta, J. R. & Weissmann, M. B. Barkhausen pulse structure in an amorphous ferromagnet: characterization by high-order spectra. *Phys. Rev. E* **57**, 6363–6369 (1998).
123. Alessandro, B., Beatrice, C., Bertotti, G., & Montorsi, A. Domain-wall dynamics and Barkhausen effect in metallic ferromagnetic materials. 1. Theory. *J. Appl. Phys.* **68**, 2901–2907 (1990).
124. Alessandro, B., Beatrice, C., Bertotti, G. & Montorsi, A. Domain-wall dynamics and Barkhausen effect in metallic ferromagnetic materials. 2. Experiment. *J. Appl. Phys.* **68**, 2908–2915 (1990).
125. Walsh, B., Austvold, S. & Proksch, R. Magnetic force microscopy of avalanche dynamics in magnetic media. *J. Appl. Phys.* **84**, 5709–5714 (1998).
126. Kryscak, L. C. & Maynard, J. D. Evidence for the role of propagating stress waves during fracture. *Phys. Rev. Lett.* **81**, 4428–4431 (1998).

## Acknowledgements

The perspective on this field described in this paper grew out of a collaboration with M. Kuntz. We thank A. Mehta for supplying the data for Fig. 7b, and D. Dolgert, M. Newman, J.-P. Bouchaud, L. C. Kryscak, D. Fisher and J. Thorpe for helpful comments and references. This work was supported by NSF grants, the Cornell Theory Center and IBM.

# The Back Page

## The Mother (Nature) of All Wars? Modern Wars, Global Terrorism, and Complexity Science

by Neil F. Johnson

It has become hard for us to watch a nightly news bulletin without hearing phrases such as “thirty dead in Iraq,” “five wounded in Afghanistan,” “three guerrilla attacks in Colombia,” or “ten killed in a terrorist bomb in Indonesia.” We are then typically presented with a number of studio experts who try to explain away the numbers by drawing on idiosyncratic details of the conflict in question. Although often unconvincing, their approach is perfectly defensible given the very different origins, motivations, locations and durations of these separate conflicts. However recent research by a multi-disciplinary team of Complexity scientists suggests that all these sociological, political and strategic experts may have missed something crucial.

Using techniques from the physics of Complex Systems, the research team has shown that the dynamics underlying all such modern conflicts, including global terrorism, are remarkably universal. Furthermore they have developed a physics-based theory describing the dynamics of insurgent group formation and attacks, which neatly explains the universal patterns observed in all modern wars and terrorism. The implications are quite sobering: Regardless of the origins and locations of modern conflicts, the insurgent groups in each case are operating in the same way. In short, it is effectively the same enemy on all fronts.

There are two reasons why the field of human conflict should be of interest to a physicist. First, the increased availability of computerized datasets means that there is a data revolution underway across the social sciences—just as the field of astronomy recently caught alight as a result of improved data collection. Human conflict is as old as mankind itself—however, a lack of reliable time-series data in the past has kept it out of reach of the quantitative sciences. This has now changed with the media, governments and non-governmental organizations all now regularly collecting data on ongoing conflicts. Admittedly the analysis of their datasets is not always straightforward—not only do the individual agencies differ in their numbers, but the way in which the figures are reported can differ quite markedly. Extensive cross-checks from the various sources must therefore be carried out prior to any data analysis.

The second reason touches the fascinating aspect of Complexity Science itself. In particular, modern wars seem to exhibit all the common characteristics of Complex Systems: (1) There is feedback, both at the microscopic and macroscopic scale, yielding a system with memory and non-Markovian dynamics. (2) The time-series of events is non-stationary. (3) There are many types of “particle,” according to the various armed actors, and they interact in possibly time-dependent ways. The war’s evolution is then driven by this ecology of agents. (4) The agents can adapt their behavior and decisions based on past outcomes. The system is far from equilibrium and can exhibit extreme behavior—for example, if the strategies of several groups of agents suddenly coincide. (5) The observed war constitutes a single realization of the system’s possible trajectories. (6) The system is open, with this coupling to the environment making it hard to distinguish between exogenous (i.e. outside) and endogenous (i.e. internal, self-generated) effects.

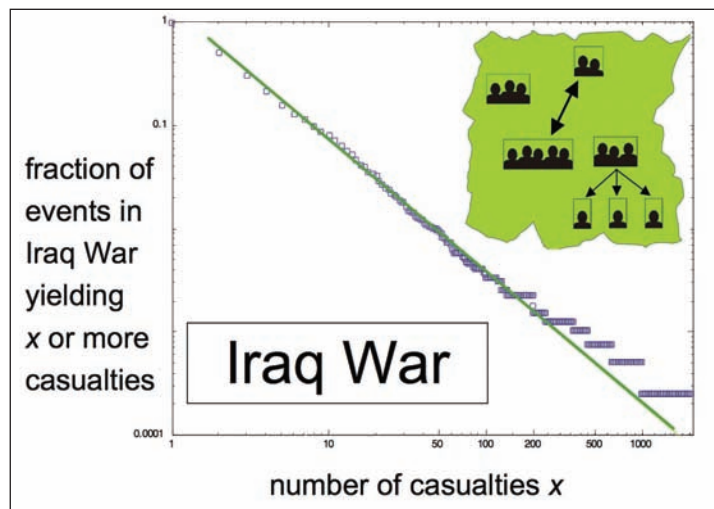
Mike Spagat from the University of London, Jorge Restrepo and Roberto Zarama in Bogota, Colombia, and I have compiled, cross-checked and analyzed event datasets for a wide variety of ongoing and recent wars, including acts of global terrorism. In each case, we plotted the histogram of the number of events within a given war with  $x$  or more casualties, versus  $x$ , on a log-log plot. What we found was really quite startling. Although wars are the antithesis of an ordered system, the datapoints for each war fell neatly on to a straight line (see the figure). This suggests a power-law behavior, which we then confirmed statistically. We repeated this exercise for wars as diverse as Israel, Senegal, Peru, Afghanistan and Colombia. In each case we obtained a power-law, i.e. the fraction of events with  $x$  casualties varies as  $x^{-\alpha}$ . This finding is remarkable given the different conditions, locations and durations of these separate wars. For example, the Iraq war is being fought in the desert and cities and is fairly recent, while the twenty-year old Colombian war is being fought in mountainous jungle regions against a back-drop of drug-trafficking and Mafia activity. This power-law finding also has some very important practical implications in terms of military planning,

high attack strength. When a given attack unit undertakes an attack, it creates a number of casualties proportional to its strength—hence the distribution of attack-unit strengths will reflect the distribution of casualties which arise in the war.

When our model is solved analytically, it produces a power-law with  $\alpha = 2.5$ . If we then make the group formation-dissociation probabilities depend on the existing group sizes, this  $\alpha$  value can be moved toward 2.0 or 3.0, thereby incorporating all the results for modern wars. Generalizing the model further to include multiple insurgent groups, yields a near-perfect fit with the real data over the entire range of  $x$ , including the nonlinear deviations at high and low  $x$ . Hence we can explain the entire range of casualty events in all modern wars and terrorism using slight variations of the same basic model.

While outside the realm of traditional physics, this new line of physics research has led to a novel quantitative understanding of current world conflicts, terrorism and insurgent warfare. In particular, it suggests that the dynamics of insurgent group formation are the same across all arenas—from the jungles of Colombia through to the deserts of Iraq, and including the entire world stage of global terrorism. In short, the way in which modern wars and terrorism are being waged has less to do with geography or ideology, and more to do with the day-to-day mechanics of human insurgency—in other words, it is simply the way in which insurgent groups of human beings fight when faced with a much stronger, but more rigid, opponent. As a consequence of this, it would seem that unless the stronger, but more rigid, opponent can change its tactics, the same statistical patterns of casualties will be repeated indefinitely into the future.

What about the future of this research? Having looked at event sizes, we are now focusing on their timing—not only in ongoing wars, but also in organized crime activity including homicides, kidnappings and extortion. With the help of Sean Gourley, Juan Camilo Bohorquez and Elvira Restrepo at the Universidad de Los Andes in Colombia, we have successfully created multi-agent models which mimic the decision-making dynamics of insurgent groups, just as had been done earlier for groups of financial traders within the so-called Econophysics community (see *Financial Market Complexity* (Oxford University Press, 2003)). By analyzing the size, timing and spatial coordinates of a given event, as well as the groups involved, we are now able to reconstruct the possible trails which a particular insurgent group might have followed. Just as in a multi-species ecological setting within the natural world, we are interested in determining the behaviors and possible protocols which arise when a particular group from insurgent army A happens to cross the path of a particular group from insurgent army B. In particular, we are trying to deduce whether they decide to fight each other, collaborate, ignore each other—or even consciously avoid each other. Going further, we know that wars like the ones in Colombia and Afghanistan have taken place against the backdrop of an illicit trade such as drug trafficking. This activity provides an effective nutrient supply in the form of money for buying supplies and weapons, and thereby helps feed the war as a whole. So just like a fungus will thrive in a forest, or a cancer tumour will thrive in a host, these armed groups are fed by a rich source of nutrients which allows them to self-organize into a robust structure. Admittedly, just like a jungle itself, this is all very far from our everyday experiences as physicists. But the exciting news is that the tools to help answer such unlikely questions are now beginning to emerge—and they are emerging from a very unlikely source: Physics.



Log-log plot of the fraction of all events in the Iraq War with  $x$  or more casualties, versus  $x$ . Squares are actual war data. The line is produced by the physics-based analytic model (see inset). All modern wars, including terrorism, show power-law like behavior with exponents in the vicinity of 2.5. The analytic model considers insurgent armies as an ecology of attack units, which undergo frequent coalescence and fragmentation. The number of dark shadows is proportional to the number of casualties which each attack unit can typically inflict in a conflict event. Full details are given in e-print “Universal patterns underlying ongoing wars and terrorism,” by Neil F. Johnson, Mike Spagat, Jorge A. Restrepo, Oscar Becerra, Juan Camilo Bohorquez, Nicolas Suarez, Elvira Maria Restrepo, Roberto Zarama, which is available at <http://xxx.lanl.gov/abs/physics/0605035>

It means there is no typical size of event—unlike the bell-curve for population heights, for example, which is centered around an average height. Deadly events with many casualties will occur—rarely, but they will occur. This is again unlike the case of heights, where the chances that someone will be taller than ten feet are truly negligible.

But the surprises don't stop there. Not only did we obtain straight-line slopes, but these slopes all produced a power-law exponent  $\alpha$  near 2.5. Furthermore Aaron Clauset and co-workers recently analyzed an extensive database of global terror events, and also obtained a power-law—with an  $\alpha$  value equal to 2.5. By contrast when we looked at data from older wars—such as the civil wars in the US, Spain and Russia—we found no statistical evidence for a power-law at all. Furthermore, the power-law exponent is insensitive to any systematic over- or under-reporting of casualties, because the overall number of casualties is just a normalizing factor. Hence the power-law signature successfully focuses on the war's internal pattern of events and hence casualties, as opposed to simply monitoring the aggregate number.

But why should 2.5 be such a magic number for modern wars and global terrorism? To answer this, we developed a model of dynamical group-formation to describe an insurgent force. Our cue came from the fact that most modern wars, including terrorism, can be characterized by an asymmetric ‘David-and-Goliath’ structure in which a small, but agile, insurgent force faces a much stronger, but more rigid, institutional force such as a state’s army. Because of its less rigid structure, the insurgent force is able to self-organize itself into a loosely connected soup of attack units which combine and dissociate over time in response to their own ad hoc operations, and in response to the state army’s operations. These attack units are shown in the inset in the figure. The number of dark shadows in each unit is proportional to the number of casualties that that unit will inflict in a typical conflict event. Each attack unit comprises a group of people, weapons, explosives, machines, or even information, which temporarily organizes itself to act as a single unit. In the case of people, this means that they are probably connected by a common location, or by some common communication system. However, an attack unit may also consist of a combination of people and objects—for example, explosives plus a few people, such as in the case of suicide bombers. Such an attack unit, while only containing a few people, could have a high attack strength. Information could also be a valuable part of an attack unit. A lone suicide bomber who knows when a certain place will be densely populated—for example a military canteen at lunchtimes—and who knows how to get into such a place unnoticed, will also represent an attack unit with a

Neil Johnson is a Professor of Physics at Oxford University, where he runs a research group focusing on complex systems in the classical and quantum domains. See “*Financial Market Complexity*,” (Oxford University Press, 2003) and “*Two's Company, Three is Complexity*” (Oneworld Publishing, 2007) for more details.

